

**Zero-field thermopower of a thin heterostructure membrane with a two-dimensional electron gas**

M. Schmidt, G. Schneider, Ch. Heyn, A. Stemann, and W. Hansen

*Institut für Angewandte Physik und Zentrum für Mikrostrukturforschung, Jungiusstraße 11, D-20355 Hamburg, Germany*

(Received 23 September 2011; revised manuscript received 13 December 2011; published 13 February 2012)

We study the low-temperature thermopower of micrometer-sized free-standing membranes containing a two-dimensional electron system. Suspended membranes of 320 nm thickness, including a high-electron-mobility structure in the Hall bar geometry of  $34\ \mu\text{m}$  length are prepared from GaAs/AlGaAs heterostructures grown by molecular-beam epitaxy. Joule heating on the central region of the membrane generates a thermal gradient with respect to the suspension points where the membrane is attached to cold reservoirs. Temperature measurements on the membrane reveal strong thermal gradients due to the low-thermal conductivity. We measure the zero-field thermopower and find that the phonon-drag contribution is suppressed at low temperatures up to 7 K.

DOI: [10.1103/PhysRevB.85.075408](https://doi.org/10.1103/PhysRevB.85.075408)

PACS number(s): 72.15.Eb, 73.50.Lw, 73.61.Ey

**I. INTRODUCTION**

Nanowires and thin membranes have attracted much attention in the field of thermoelectrics because their thermal conductivities are reduced by several orders of magnitude compared to bulk material.<sup>1–3</sup> There are several papers on the thermal properties of microscaled structures as, for example, GaAs microbars<sup>3,4</sup> and Si nanowires.<sup>5,6</sup> In recent years, many papers were published on the thermopower of such nanowires, and it became common practice to prepare the nanowires in a free-standing fashion<sup>5</sup> to decouple the wires from the substrate avoiding heat losses to or influences from the latter. Thermopower studies that have been performed on two-dimensional electron gases (2DEGs) in heterostructures on bulk substrates still show strong interactions of the electronic system with the substrate.<sup>7–9</sup> Here, we report about thermopower studies of suspended 2DEGs.

Thermoelectric studies of 2DEG systems started shortly after the discovery of the quantum Hall effect<sup>10</sup> and attracted considerable interest since then.<sup>7,11–16</sup> Generally, a thermal gradient established by Joule heating along a macroscaled sample is used to investigate the thermopower associated with the temperature drop between the voltage probes. Then, two effects are expected to contribute to the thermopower, the thermodiffusion, and the phonon drag. It is of interest how their influence might be modified in suspended nanostructures. Phonon-drag thermopower is found to dominate in a temperature range that starts at very low temperatures, i.e., below  $T = 1\ \text{K}$  in bulk GaAs.<sup>7,8</sup> Different efforts were made to experimentally separate the diffusion thermopower and the phonon-drag contribution. Ying *et al.*<sup>8</sup> used a GaAs substrate that was thinned to  $100\ \mu\text{m}$ . They were able to measure the pure thermodiffusion of a 2D hole gas at temperatures below 100 mK. Fletcher *et al.*<sup>9</sup> used a heavily doped substrate and suppressed the phonon drag up to 0.5 K. Finally, the use of direct-heating techniques of the 2DEG reduces the thermal gradient in the lattice and suppresses the phonon drag in the electronic system. This way it has been possible to study the diffusion thermopower up to a temperature of  $T = 2\ \text{K}$ , which is the highest value reported for GaAs yet.<sup>17,18</sup>

We present thermopower measurements on suspended microscaled 2DEGs confined in a thin GaAs/AlGaAs heterostructure membrane as shown in Fig. 1. The sample setup

combines the advantageous properties of drastically reduced heat conductivity of free-standing thin membranes and the high electric conductivity of 2DEGs. While electrical transport properties of 2DEGs embedded in thin membranes have been studied in several papers,<sup>19–22</sup> thermal transport rarely is reported, and so far, thermopower measurements are missing. We demonstrate that, in our membranes, the thermal transport of the lattice is reduced strongly due to the small dimensions. This allows us to establish strong thermal gradients along the 2DEG even at distances of only several micrometers, which is not possible on structures in contact with bulk GaAs.<sup>1,2</sup> With our structure, we observe that the small dimensions strongly affect the thermopower suppressing the phonon drag in the 2DEG up to temperatures of 7 K.

**II. EXPERIMENT**

The measurements were carried out on a free-standing membrane containing an electron system in a high electron mobility (HEMT) structure that is shown in Fig. 1. The thickness of the membrane is 320 nm, and the length is  $100\ \mu\text{m}$ . The lateral dimension of the membrane is about 2 orders of magnitude smaller than samples used in previous papers of thermoelectric studies on 2DEGs in GaAs heterostructures.<sup>7,10,12,23</sup>

The samples were fabricated using solid-source molecular-beam epitaxy (MBE) on (001) GaAs substrates. A 500 nm-thick  $\text{Al}_{0.61}\text{Ga}_{0.39}\text{As}$  sacrificial layer is followed by the HEMT structure with a 350 nm layer of intrinsic GaAs, a 30 nm  $\text{Al}_{0.35}\text{Ga}_{0.65}\text{As}$  spacer layer, a 57 nm  $\text{Si:Ga}_{0.65}\text{Al}_{0.35}\text{As}$  doping layer, and a 5 nm GaAs cap. A 2DEG is formed at the GaAs/ $\text{Al}_{0.35}\text{Ga}_{0.65}\text{As}$  interface.

We used electron-beam lithography to structure a  $34\ \mu\text{m}$ -long micro-Hall bar, a metal heater placed in the center of the membrane for Joule heating of the crystal lattice, and two thermometers at the ends of the Hall bar as shown in Fig. 1. Joule heating of the wound heater generates a temperature gradient directed along the membrane. A 120 nm etching step defines the Hall bar containing the 2DEG and leaves the rest of the membrane semi-insulating. All leads as well as the thermometers and the heater were fabricated in one evaporation step so that all metallizations can be assumed to have the same specific resistivity. From the specific resistivity,

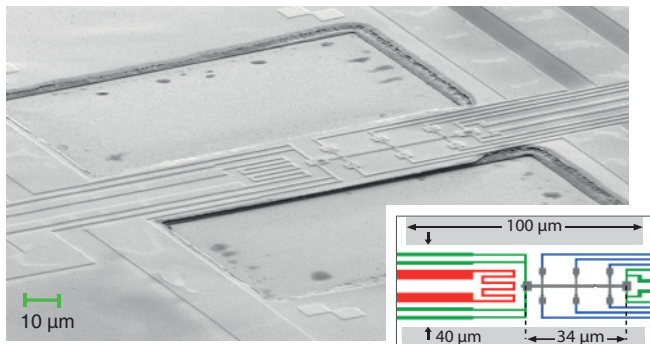


FIG. 1. (Color online) Scanning electron micrograph of a suspended 320 nm-thick, 40  $\mu\text{m}$ -wide, and 100  $\mu\text{m}$ -long GaAs membrane with a 34  $\mu\text{m}$ -long Hall bar device composed of a GaAs/AlGaAs heterostructure containing a 2DEG. The inset shows a schematic of the membrane (white) with color-coded features and sample dimensions. A microheater (red) and thermometers (green) enable the generation and the measurement of the temperature drop directed along the Hall bar (gray), respectively.

we determine the resistance of the wound-heating wire in order to calculate the heater power from the heater current. In this paper, AuGe with a small content of  $\approx 5\%$  Ni was used to benefit from the Kondo effect enhancing the sensitivity of the thermometers at low temperatures. We also tested pure Au as a metal with significantly lower specific resistivity compared to AuGeNi and could exclude any influence of the chosen metal on the measured thermopower. The film thickness of the evaporated metal was 40 nm. Finally, chemical wet etching of the mesa with  $\text{H}_3\text{PO}_4/\text{H}_2\text{O}_2/\text{H}_2\text{O}$  and selective wet etching of the  $\text{Al}_{0.61}\text{Ga}_{0.39}\text{As}$  sacrificial layer with a 5% solution of hydrofluoric acid detaches the membrane from the substrate. In the suspended membrane, we determine a carrier density of the 2DEG of  $n_s = 1.3 \times 10^{11} \text{ cm}^{-2}$ . The mobility of the 2DEG in the detached membrane is about  $97\,000 \text{ cm}^2 \text{ V}^{-1} \text{ s}^{-1}$ .

The thermometers at the hot and cold ends of the Hall bar are designed in four-point geometry. Both thermometers were calibrated at an equilibrium condition in a slow-bath-temperature sweep. The calibration curves for both thermometers are shown in the inset of Fig. 2. Whereas, in the thermometers made of pure Au, the saturation of the resistivity does not allow for temperature measurements below 10 K, the Kondo effect in the AuGeNi thermometers allows for temperature measurements down to the lowest temperature of 1.3 K available in our cryostat.

In addition, both thermometers act as ohmic contacts to the 2DEG by the use of segregated NiAuGe, so we can guarantee that the position at which the thermovoltage is measured can be associated with a precise temperature at the membrane. Furthermore, the segregated NiAuGe thermally anchors the electron temperature to the crystal lattice. We note that, in the temperature range  $T > 65 \text{ K}$ , the thermometers become less accurate. There, the thermometer resistances reach minimum values (see the inset of Fig. 2), and the error in the measured thermal conductivity values increases to approximately 10%.

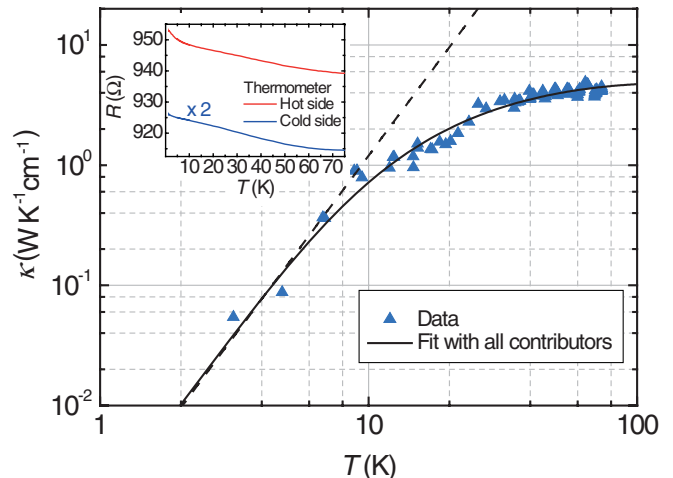


FIG. 2. (Color online) Thermal conductivity  $\kappa$  of a membrane with  $42 \mu\text{m} \times 320 \text{ nm}$  cross-sectional area. The solid line is calculated via the Callaway model. The dashed line is a function proportional to  $T^3$  demonstrating the influence of the phonon-specific heat at low temperatures. The inset shows the run of the thermometer resistances of the hot (red) and cold (blue, multiplied by 2 for better comparison) end side thermometer, respectively, which we used for calibration.

### III. THERMAL CONDUCTIVITY

The measurements were performed using a variable-temperature cryostat. For the measurement of the thermal conductivity, we apply Joule heating to the heater and measure the temperature drop between the thermometers. As the suspension points of the membrane act as the heat sinks, a thermal gradient is established along the membrane. When a steady state is achieved, the heat flow along the membrane causes a constant temperature gradient between the thermometers, and the thermal conductivity of the membrane can be determined by the temperature difference  $\Delta T$  of the thermometers and the heater power  $P$  as

$$\kappa = \frac{P}{\Delta T} \frac{\Delta x}{A}, \quad (1)$$

where  $\Delta x$  is the distance between the thermometers and  $A$  is the cross-sectional area of the membrane. Here, we neglect radiation loss, which is extremely small at the temperatures of our measurement. The heating power  $P$  is calculated assuming a temperature-independent heater resistivity of 5 k $\Omega$ . This assumption is associated with a small error below 2% because of the small temperature dependence of the metal.

We determined the thermal conductivity in a temperature range between 3 and 75 K as shown in Fig. 2. The run of the thermal conductivity can be described well by a model developed by Callaway.<sup>25</sup> We use this model with later corrections that can, e.g., be found in the publication of Fon *et al.*<sup>3</sup> and investigate the effects of phonon-boundary, phonon-electron, phonon-defect, and phonon-Umklapp scattering on the thermal conductivity of our membrane. The different phonon-scattering mechanisms enter into the model with their corresponding relaxation times, which are combined

in the total relaxation time  $\tau$  according to Matthiessen's rule,

$$\begin{aligned}\tau^{-1} &= \tau_{\text{bound}}^{-1} + \tau_{\text{electron}}^{-1} + \tau_{\text{defect}}^{-1} + \tau_{\text{phonon}}^{-1} \\ &= c_{\text{av}}/\Lambda_{\text{bound}} + \alpha\nu + \beta\nu^4 + \gamma\nu^2 T e^{-(\Theta_D/3T)},\end{aligned}\quad (2)$$

with the phonon frequency  $\nu$ , the Debye temperature  $\Theta_D$ , and the average phonon group velocity  $c_{\text{av}} \approx 3500$  m/s. Fitting parameters are  $\alpha$ ,  $\beta$ ,  $\gamma$  and  $\Lambda_{\text{bound}}$ . The latter represents the limiting phonon mean-free path (mfp) for diffusive boundary scattering. The linear form of the phonon-electron-scattering rate is adequate for scattering in a degenerate semiconductor,<sup>26</sup> and the fourth-power dependence of the defect-scattering rate is commonly used for Rayleigh scattering at point defects.<sup>27</sup>

Thus, from a fit with the Callaway model, we obtain information about the rates of different phonon-scattering mechanisms and their contribution to the thermal resistivity of the membrane. The parameters extracted from the fit in Fig. 2 are  $\Lambda_{\text{bound}} = 67.24 \mu\text{m}$ ,  $\alpha = 6.68 \times 10^{-28}$ ,  $\beta = 2.43 \times 10^{-41} \text{ s}^3$ , and  $\gamma = 1.73 \times 10^{-18} \text{ s/K}$ . In comparison to bulk values where  $\Lambda_{\text{bound}}$  is usually on the order of millimeters, diffusive phonon-boundary scattering in the membrane is enhanced strongly.<sup>1,2</sup> This can be understood easily in view of the drastically reduced cross-sectional area of the thin membrane. The dashed line in Fig. 2 is a function proportional to  $T^3$ , which reflects the thermal conductivity as expected due to the Debye phonon heat capacity at low temperatures. At these temperatures, only boundary scattering gives the limiting factor to  $\kappa$  so that the phonon mfp can be assumed to be constant.

Furthermore, according to the fit results, phonon-electron scattering gives a negligible contribution to the thermal resistivity. This can be explained with the membrane setup that contains free charge carriers only in the spatially confined plane of the 2DEG in combination with the dominance of boundary and defect scatterings in the structure.

We find that the value of  $\beta$  for defect scattering deduced from the fit is on the order of those measured in bulk GaAs, indicating that the rate of point-defect scattering is not significantly changed in our membrane.<sup>27</sup> Phonon-defect scattering is responsible for the reduced rise in  $\kappa$  at temperatures above 10 K.

The value of  $\gamma$  for phonon-phonon Umklapp scattering in our membrane is about an order of magnitude smaller than bulk values. From the result of the Callaway model, we expect that phonon-Umklapp scattering will gain influence in the membrane not below 100 K. This is in contrast to bulk GaAs where Umklapp-scattering processes already become dominant at temperatures above 10 K.<sup>1,2</sup>

We note that the run of the thermal conductivity of our membrane is comparable to thermal conductivities determined in an earlier paper by Fon *et al.*<sup>3</sup> on GaAs nanobars of  $200 \text{ nm} \times 200 \text{ nm}$  cross-sectional area. The thermal conductivities for those membranes are reduced by 2 orders of magnitude, which we attribute to the 2 orders of magnitude larger width of our membrane with respect to the nanobars studied by Fon *et al.*

In addition to the phonons, the electrons in the leads and the Hall bar contribute to the thermal conductivity  $\kappa$  of the membrane. This contribution can be estimated via the

Wiedemann-Franz law as  $\kappa_{\text{WF,lead}} = L_0 \sigma_{\text{lead}} T$  and  $\kappa_{\text{WF,2DEG}} = L_0 \sigma_{\text{2DEG}} T$  with the Lorentz number  $L_0$  and the specific electrical conductivities  $\sigma_{\text{lead}}$  and  $\sigma_{\text{2DEG}}$  of the leads and the 2DEGs, respectively.<sup>24</sup> However, with  $\kappa_{\text{WF,lead}} + \kappa_{\text{WF,2DEG}} < 0.01 \text{ W cm}^{-1} \text{ K}^{-1}$  in the temperature range  $T < 75 \text{ K}$ , the thermal conductivities of the leads and the 2DEG are negligible compared to the measured thermal conductivities.

#### IV. THERMOPOWER

Utilizing the low thermal conductivity of the membrane compared to bulk material, the thermopower  $S$  was determined at temperatures between 2.7 and 14 K without an external magnetic field. We use the ohmic contacts of the thermometers to the 2DEG to measure the thermovoltage over the full length of the 2DEG ( $34 \mu\text{m}$ , see Fig. 1) and to calculate the thermopower with the temperature drop determined by the thermometers. The thermopower  $S = S_d + S_{\text{ph}}$  arises from two contributions, the charge carrier diffusion  $S_d$  and the so-called phonon drag  $S_{\text{ph}}$ .<sup>14,28</sup> The latter is caused by the phonon wind from which momentum is transferred to the charge carriers. To calculate the diffusion thermopower  $S_d$ , we assume the Mott formula<sup>14,29,30</sup> to be a good approximation for temperatures below 20 K,

$$S_d = -\frac{\pi^2 k_B^2 T}{3e E_F} (p - 1). \quad (3)$$

The diffusion thermopower, thus, is proportional to the ratio of the temperature to the Fermi temperature of the electronic system. Furthermore, it depends on the parameter  $p$  that takes account of the energy dependence for the carrier-scattering time. As in previous papers,<sup>7,14</sup> we assume that the electronic conductivity can be expressed in terms of an energy-dependent relaxation time  $\tau = \tau_0 E^p$ , where  $E$  is the electron energy,  $\tau_0$  is a function of temperature (but independent of  $E$ ), and the power factor  $p$  is the parameter occurring in Eq. (3). The power factor, in turn, depends on the scattering mechanisms at work.

The dashed line in Fig. 3 is calculated with the experimental carrier density of  $1.3 \times 10^{11} \text{ cm}^{-2}$  yielding a Fermi energy of 4.7 meV, which is related to a Fermi temperature of 55 K. The slope corresponds to a power factor of  $p = -0.5$ . In previous papers on AlGaAs-GaAs HEMT structures, the factor  $p$  was found mostly to be on the order of unity.<sup>12,13</sup> It was associated with remote and background impurity scatterings. However, the carrier densities were much larger in those papers compared to the carrier density in our sample. Different scattering mechanisms are dominant at different charge carrier densities  $n$  so that  $p$  also depends on  $n$ . Karavolas and Butcher<sup>31</sup> calculated the parameter  $p$  in the carrier density range from 5 to  $12 \times 10^{11} \text{ cm}^{-2}$  for HEMT structures on bulk substrates. They considered interface roughness and remote and background impurities and found that, in this carrier range,  $p$  can take values between  $-1.5$  and  $1.5$ . In our sample, scattering due to strain fields and even dislocations may occur after the suspension of the membrane so that additional scattering mechanisms influence the parameter.

In Hall bars on bulk GaAs substrates, the phonon drag dominates the thermopower already in the sub-Kelvin range.<sup>7,12</sup> In contrast, in our membrane, the diffusion thermopower dominates up to much higher temperatures. The temperature

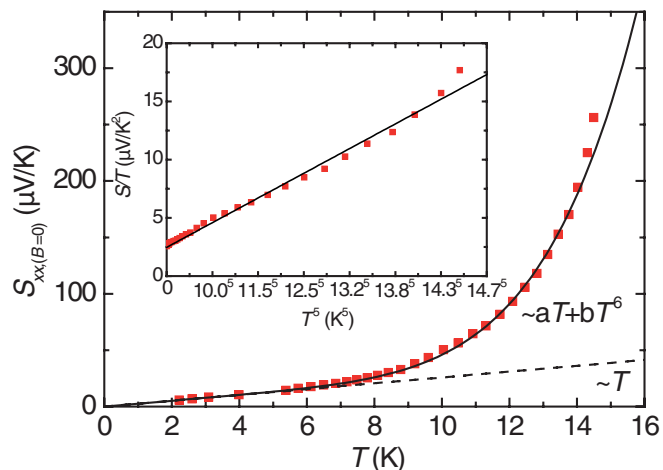


FIG. 3. (Color online) Temperature dependence of the zero-field thermopower. The dashed line illustrates the diffusion part of the thermopower  $S_d$  calculated via the Mott formula with the experimental electron density and a power factor of  $p = -0.5$ . The solid line represents the total thermopower calculated as  $S = S_d + S_{ph}$ . The inset shows a plot of  $S/T$  vs  $T^5$  together with a fit  $\propto T^5$ . The intercept of the fit at  $T = 0$  is at  $2.2 \mu\text{V}/\text{K}^2$ .

dependence of the phonon-drag thermopower  $S_{ph}$  generally is taken to be of the form  $S_{ph} \propto \Lambda T^n$ , with  $\Lambda$  being the phonon mfp and an exponent  $n$  that is 4 or 6 for electron-phonon coupling by piezoelectric or by deformation-potential interaction, respectively.<sup>14,32,33</sup>

The solid line in Fig. 3 represents a fit to the total thermopower calculated as  $S = S_d + S_{ph} = aT + bT^6$  with the parameter  $a = 2.47 \mu\text{V}/\text{K}^2$  obtained from Eq. (3). The best fit is obtained when we take a constant phonon mfp, which yields the fitting parameter  $b = 2.12 \times 10^{-5} \mu\text{V}/\text{K}^7$ . Interestingly, the calculation agrees even for temperatures higher than 10 K where the mfp  $\Lambda$ , determined from the run of the thermal conductivity, starts to become strongly  $T$  dependent. We note that the introduction of an additional  $T^4$  term to the fit results in a less accurate matching with the measured data.

In our suspended structure, the phonon-drag contribution starts to dominate the total thermopower beyond 7 K where the thermopower deviates from the linear run as obvious in Fig. 3. The inset of Fig. 3 shows a plot of  $S/T$  vs  $T^5$  together with a calculated fit proportional to  $T^5$ . The intercept at  $T = 0$  is at  $2.2 \mu\text{V}/\text{K}^2$  in good correspondence with the value calculated by the Mott formula.

In previous papers on thermopower studies with HEMTs on bulk GaAs crystals, the phonon drag sets in at much

lower temperatures. Furthermore, the temperature dependence is described by an exponent  $3 \leq n \leq 4$  instead of  $n = 6$ .<sup>7,16</sup> From this, it was concluded that phonon drag was dominated by piezoelectric phonon-electron coupling in HEMTs on bulk GaAs. The  $n = 6$  power law observed in our HEMTs on thin membranes, thus, might indicate a different coupling mechanism. We note, however, that for a quantitative analysis, it must be considered that the contact separation is on the scale of the phonon mfp. In all previous papers where lattice heating was applied to generate a thermal gradient,<sup>7,8,12,13,18,28</sup> the devices were macroscaled with lengths that were several times the phonon mfp. This indicates that the small contact separation is responsible for the fact that the phonon-drag signal in our device is much smaller than in macroscopic samples of previous papers.

## V. CONCLUSION

In conclusion, we used a suspended GaAs membrane to establish strong temperature gradients along a microscaled Hall bar containing a 2DEG. From the temperature gradient, the thermal conductivity of the membrane was determined. Below 20 K, it was found to be up to 2 orders of magnitude smaller than GaAs bulk values. Furthermore, the run was similar to data for microscaled GaAs structures previously reported.<sup>3</sup> The zero-field thermopower of the low-dimensional electron gas was found to be dominated by thermodiffusion in the low-temperature range up to 7 K. This temperature was significantly larger than previously reported values for non-suspended HEMT structures. The phonon-drag thermopower was found to be strongly suppressed with respect to HEMTs on bulk GaAs substrates, and an  $n = 6$  power law was observed for the temperature dependence. We attributed the observations to the small dimension of the membrane in combination with the small distance between the contacts of the device. The  $n = 6$  power law might indicate a different electron-phonon coupling in the suspended membrane as compared to bulk samples. The small contact separation, which was on the order of the phonon mfp, led to a suppression of the phonon-drag signal. A theoretical model is needed to reveal how the small contact separation influences the temperature dependence of the phonon-drag contribution to the thermopower.

## ACKNOWLEDGMENTS

The authors thank the Deutsche Forschungsgemeinschaft for financial support via SPP 1386 “Nanostructured Thermoelectrics.”

<sup>1</sup>R. O. Carlson, G. A. Slack, and S. J. Silverman, *J. Appl. Phys.* **36**, 505 (1965).

<sup>2</sup>M. G. Holland, *Phys. Rev.* **132**, 2461 (1964).

<sup>3</sup>W. Fon, K. C. Schwab, J. M. Worlock, and M. L. Roukes, *Phys. Rev. B* **66**, 045302 (2002).

<sup>4</sup>T. S. Tighe, J. M. Worlock, and M. L. Roukes, *Appl. Phys. Lett.* **70**, 2687 (1997).

<sup>5</sup>A. I. Hochbaum, R. Chen, R. D. Delgado, W. Liang, E. C. Garnett, M. Najarian, A. Majumdar, and P. Yang, *Nature (London)* **451**, 163 (2008).

- <sup>6</sup>A. I. Boukai, Y. Bunimovich, J. Tahir-Kheli, J.-K. Yu, W. A. Goddard III, and J. R. Heath, *Nature (London)* **451**, 168 (2008).
- <sup>7</sup>For an overview, please refer to B. L. Gallagher and P. Butcher, *Handbook on Semiconductors* (Elsevier Science, New York, 1992), p. 721.
- <sup>8</sup>X. Ying, V. Bayot, M. B. Santos, and M. Shayegan, *Phys. Rev. B* **50**, 4969 (1994).
- <sup>9</sup>R. Fletcher, P. T. Coleridge, and Y. Feng, *Phys. Rev. B* **52**, 2823 (1995).
- <sup>10</sup>H. Obloh and K. v. Klitzing, *Surf. Sci.* **142**, 236 (1984).
- <sup>11</sup>T. M. Fromhold, P. N. Butcher, G. Qin, B. G. Mulimani, J. P. Oxley, and B. L. Gallagher, *Phys. Rev. B* **48**, 5326 (1993).
- <sup>12</sup>R. Fletcher, J. J. Harris, C. Foxon, M. Tsousidou, and P. Butcher, *Phys. Rev. B* **50**, 14991 (1994).
- <sup>13</sup>B. R. Cyca, R. Fletcher, and M. D'Iorio, *J. Phys.: Condens. Matter* **4**, 4491 (1992).
- <sup>14</sup>N. Sankeshwar, M. Kamatagi, and B. Mulimani, *Phys. Status Solidi B* **242**, 2892 (2005).
- <sup>15</sup>C.-H. Lee, G.-C. Yi, Y. M. Zuev, and P. Kim, *Appl. Phys. Lett.* **94**, 022106 (2009).
- <sup>16</sup>B. Tieke, R. Fletcher, U. Zeitler, M. Henini, and J. C. Maan, *Phys. Rev. B* **58**, 2017 (1998).
- <sup>17</sup>S. Maximov, M. Gbordzoe, H. Buhmann, and L. Molenkamp, *Phys. Rev. B* **70**, 121308(R) (2004).
- <sup>18</sup>W. E. Chickering, J. P. Eisenstein, and J. L. Reno, *Phys. Rev. Lett.* **103**, 046807 (2009).
- <sup>19</sup>R. H. Blick, F. G. Monzon, W. Wegscheider, M. Bichler, F. Stern, and M. L. Roukes, *Phys. Rev. B* **62**, 17103 (2000).
- <sup>20</sup>S. Mendach, O. Schumacher, C. Heyn, S. Schnll, H. Welsch, and W. Hansen, *Physica E* **88**, 274 (2004).
- <sup>21</sup>S. Mendach, O. Schumachen, H. Welsch, C. Heyn, and W. Hansen, *Appl. Phys. Lett.* **88**, 212113 (2006).
- <sup>22</sup>K.-J. Friedland, R. Hey, H. Kostial, A. Riedel, and K. H. Ploog, *Phys. Rev. B* **75**, 045347 (2007).
- <sup>23</sup>T. H. H. Vuong, R. T. Nicholas, M. A. Brummell, J. C. Portal, F. Alexandre, J. M. Masson, and T. Kerr, *Solid State Commun.* **57**, 033701 (1986).
- <sup>24</sup>R. T. Syme, M. J. Kelly, and M. Pepper, *J. Phys.: Condens. Matter* **1**, 3375 (1989).
- <sup>25</sup>J. Callaway, *Phys. Rev.* **113**, 1046 (1959).
- <sup>26</sup>J. M. Ziman, *Electrons and Phonons* (Oxford University Press, Oxford, 1960).
- <sup>27</sup>M. G. Holland, *Phys. Rev.* **134**, A471 (1964).
- <sup>28</sup>C. Ruf, H. Obloh, B. Junge, E. Gmelin, K. Ploog, and G. Weimann, *Phys. Rev. B* **37**, 6377 (1998).
- <sup>29</sup>M. Cutler and N. F. Mott, *Phys. Rev.* **181**, 1336 (1969).
- <sup>30</sup>R. J. Nicholas, *J. Phys. C* **16**, L695 (1985).
- <sup>31</sup>V. C. Karavolas and P. N. Butcher, *J. Phys.: Condens. Matter* **3**, 2597 (1991).
- <sup>32</sup>R. Fletcher, V. M. Pudalov, Y. Feng, M. Tsousidou, and P. N. Butcher, *Phys. Rev. B* **56**, 12422 (1997).
- <sup>33</sup>S. Kubakaddi, *Phys. Rev. B* **69**, 035317 (2004).